Active Cell Balancing Design Integrated With SoC Estimator In Lithium-Ion Batteries

Arif Devi Dwipayana[1,*] Riz Rifai O. Sasue [2,] Adrian Pradana[3]

[1,2,3] *Automotive Technology Department Bali Land Transportation Polytechnic*
[*]*Corresponding author. Email: arif.devi@poltradabali.ac.id*

ABSTRACT
The reliability and safety of lithium-ion batteries in electric vehicle applications significantly depend on accurate State of Charge (SOC) estimation and effective cell balancing mechanisms. This study proposes the design of an active cell balancing system integrated with an SOC estimator to improve the performance, lifespan, and thermal stability of lithium-ion battery packs. The research adopts a Research and Development (R&D) approach, involving both hardware and software design. The hardware utilizes an Arduino-based control system to monitor individual cell voltages, temperature, and current, while the software implements an algorithm for active energy redistribution among cells to achieve real-time balance. A 4S1P lithium-ion battery pack (3.7V/2500mAh per cell) was developed and experimentally tested. The results demonstrate that the integrated active balancing system effectively minimizes voltage deviation between cells and maintains uniform SOC levels, reducing overcharge and overdischarge conditions. Consequently, the proposed system enhances energy utilization efficiency and extends the operational life of the battery. The integration of SOC estimation into the active balancing control loop offers a promising approach for intelligent Battery Management System (BMS) design in electric mobility and renewable energy storage applications.

Keywords: *Lithium-ion battery, Active cell balancing, State of charge (SOC) estimator, Battery management system (BMS), Energy efficiency.*

1. INTRODUCTION

Batteries are one of the core components of electric vehicles, with an average life cycle of 5 to 8 years. Given the importance of batteries in achieving energy transition, battery modeling and degradation have been extensively studied to characterize their physical, thermal, and chemical properties [1], [2], particularly for applications in electric vehicles [3]. Currently, lithium-ion batteries remain the preferred choice for electric vehicles due to their advantages of no hydrogen emissions, no memory effect, low self-discharge rate, wide operating temperature range, small size, light weight, and ability to deliver higher power [4], [5]. To prevent lithium-ion batteries from exploding due to excessive current and voltage, they are now equipped with battery management system (BMS) technology that monitors battery conditions [6]. Another function of BMS is to convey the state of charge (SOC) and state of health (SOH) of the battery, which are important parameters for determining the level of battery aging [7], [8], [9]. Given that rechargeable lithium batteries are the most common choice for many applications, estimating the remaining battery capacity is fundamental to its management because very high or very low state of charge (SOC) conditions can permanently damage the battery and pose a safety hazard. Battery systems contain different mechanical, electrical, and electronic components. Each must be considered in the design process [10]. Battery design and layout are important because these aspects are related to cost, thermal dissipation, and the production and processing phases at the end of the battery's life. There are several design approaches, namely Cell-To-Pack (CTP) and Cell-To-Chassis (CTC). Both of these design approaches respond to the need for rapid electric vehicle manufacturing processes, while the CTP approach aims to define a complete cell pack without using intermediate modules [10], while CTC integrates the cells into the structural components of the vehicle [11]. The basic solution for cell balancing is achieved by equalizing the voltage and charge status between cells connected in a battery pack [12]. Cell balancing based on the functioning of the balancing circuit is categorized as active cell balancing and passive cell balancing.

SOC is defined as the rate of available capacity to its maximum capacity when the battery is fully charged, and describes the percentage of remaining battery capacity. Battery status monitoring and control are performed by the BMS, which uses a battery analytical model and consists of hardware and software for battery management. This includes, among other things, algorithms for determining more critical battery conditions. For electric vehicle applications, batteries must not only deliver a certain amount of energy to the drive train during operation, but also provide power in various road situations. Therefore, it is important to know the maximum power that can be delivered to and from the battery through charging or discharging, and SOC is needed to make decisions regarding its operation. Estimating battery power SOC is one of the key technologies in electric vehicles, as its accuracy directly affects energy management control strategies and electric vehicle performance, thereby impacting the reliability and cost of the electric vehicle itself. The SOC status variable cannot be measured directly due to the complex electrochemical characteristics of batteries and the high degree of non- linearity exhibited by batteries in their use. It can only be estimated using externally measurable battery terminal voltage, charging and discharging currents, etc. Furthermore, the estimation process is easily influenced by factors such as temperature, cycle time, discharge rate, voltage, noise, etc., making it difficult to accurately estimate the battery SOC in real time [13]. Reliable monitoring of the state of charge (SOC) and instantaneous capacity is essential for safe and efficient operation. Despite its importance, SOC and capacity determination remain challenging tasks because both are diverse internal conditions. The coulomb counting (CC) method is known as an easy way to monitor SOC. However, as an open-loop method, it is quite susceptible to noise or drifting in the current sensor. It also depends on an accurate guess of the initial SOC, which is impossible in real- world applications [14].

Khan et al. [15] researched passive cell balancing and active cell balancing methods based on voltage and SOC as balancing criteria to determine which technique can be used to reduce inconsistencies between cells in a battery pack to increase usable capacity, thereby increasing EV range. Zhang et al. [16] presented an active cell balancing control strategy, which uses average SOC as a balancing approach and a single inductor as an energy storage component used in a buck-boost/buck-boost chopper converter. The study proposes a modular helicopter balancing circuit for energy transfer between adjacent cells that not only allows error separation but also simplifies the construction of the active cell balancing control system, making it more suitable for addressing Li-ion battery inconsistencies in electric vehicles. The research findings show that reducing the number of battery submodules decreases the balancing current and increases balancing efficiency. Adjusting the duty ratio of the power switch controls the balancing current or energy transferred in a switching cycle. It should be noted that the power rating of the series diode limits the balancing current, which increases the charging or discharging time. Buchicchio et al. [17] researched battery SOC estimation from EIS (electrochemical impedance spectroscopy) data based on machine learning and equivalent circuit models, through exploratory data analysis, showing that it is possible to distinguish different SOCs from EIS measurements. They then proposed an SOC estimation approach based on EIS and equivalent circuit models to provide a concise way to describe the frequency domain and time domain behavior of battery impedance. They experimentally validated this approach by applying it to a dataset consisting of EIS measurements performed on four cylindrical lithium-ion cells at different SOC values. The proposed approach enabled highly efficient model training and resulted in a low-dimensional SOC classification model that achieved an accuracy of over 93%. The resulting low-dimensional classification model is suitable for embedding into battery-powered systems and for online SOC estimation. Zhou et al. [18] investigated the joint estimation of SOC and SOH for lithium-ion batteries based on the particle filter Kalman fusion algorithm (MIEKPF) and extended Kalman particle filter (EKPF). The results of the study show that, first, the EKPF algorithm is applied to identify parameters and estimate SOH online, and the results of identifying resistance and capacitance parameters are used as input to compensate for errors arising from considering the effects of battery aging in estimating SOC, thereby improving the accuracy of the model. Second, the proposed combination of several new interest discrimination theories and the extended Kalman particle filtering algorithm, which takes into account the influence of past observations on current values, enables collaborative estimation of SOC and SOH throughout the Li-ion battery cycle. Finally, the MIEKPF-EKPF algorithm is compared with other existing algorithms to limit the average and maximum SOC errors to 0.48% and 2%, respectively, under New European Driving Cycle (NEDC) operating conditions. Simulation results verify the feasibility and accuracy of the proposed method.

The various advantages of Li-ion batteries have led previous research on Li-ion to focus on developing battery materials to improve specific energy, power, and cycle life rather than issues related to passive cell balancing and active cell balancing, state of charge (SOC), and state of health (SOH). Several studies have used various balancing design models to solve the problems in this research. The author developed "Integrated Active Cell Balancing Design with SOC Estimator- s in Lithium-ion Batteries" with the aim of improving SOC performance to extend the life of lithium-ion batteries.

2. LITERATURE REVIEW

The Thermal Management System or Battery Management System (BMS) is a control system in batteries that consists of one or more electronic controllers that function to regulate the charging and discharging processes, monitor the temperature and voltage in the battery and connect it to the system in electric vehicles, balance the reactions in the cells, and serve as a safety function for the battery. In Li-ion batteries, the BMS aims to protect the battery from overcharging, overdischarging, low or high temperatures, short circuits, and other types of damage. BMS is also defined as a combination of sensors, controllers, communication, and computing hardware with algorithm software designed to determine the maximum charge-discharge current and estimate the state of charge (SOC) and state of health (SOH) of the battery. SOC is defined as the remaining battery capacity and is influenced by operating conditions such as current load and temperature, while SOH is a comparison of maximum capacity, charge after use with maximum charge capacity when new. Conventional BMS has two main functions, namely monitoring and protection. The monitoring function is related to measuring current, cell voltage, and temperature, while the protection function is related to the on/off switching system depending on the existing conditions.

There are various issues to consider for the implementation of electric vehicles. Based on a literature review, the most prominent issue faced in battery-operated electric vehicles is cell balancing. Improper cell balancing in batteries also causes thermal problems in batteries [19], [20]. For passive balancing in general, the temperature increase can range from 1-2 degrees Celsius. Figure 1 shows the correct and incorrect balancing models for cell balancing in a battery pack. Intrinsic and extrinsic parameters are the main causes of cell imbalance during ideal charging and usage models, as shown in Figure 2.

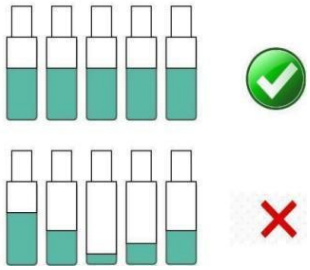

Figure 1 Proper and improper cell balancing.

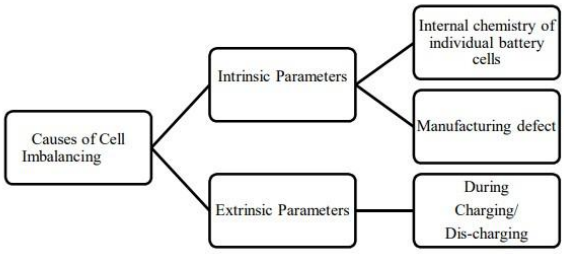

Figure 2 Causes of cell balancing in a battery pack.

Three different conditions are required for analysis: ideal mode, charging, and discharging. Battery charging varies according to the connected topology and type of use. In simple terms, cell imbalance varies according to topology and mode of use. Cell balancing is broadly classified into passive (passive cell balancing) and active (active cell balancing) based on the balancing method. Additionally, cell balancing is also classified based on the battery pack connection topology for various charging modes. The different battery equalization controller topologies used are shown in Figure 3.

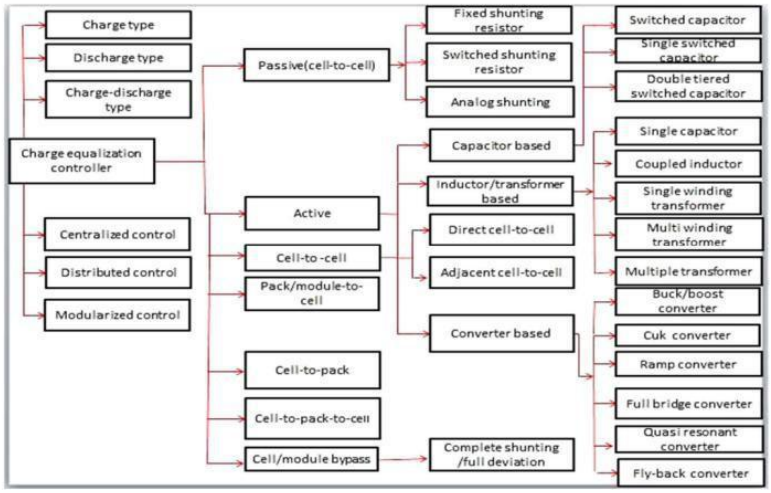

Figure 3 Battery equalization converter topology.

Cell balancing techniques based on their configuration are listed in Figure 4. This classification explains the time, size, cost, and efficiency of the topology for cell imbalance techniques [21].

Table 1. Cell balancing topologies

No.	Topology	Advantages	Disadvantages
1	Cell-By-pass	Higher Efficiency, Higher Speed, Lower Control Complexity, Smaller Size, Lower Switch Voltage Stress	Higher Current Stress across switches, Low Power Applications
2	Cell-to-Cell	Higher Efficiency, Lower Complexity, Lower Balancing Time, High Power Application	Higher Voltage Stress across switches, Larger Size, More Expensive, Higher Current Stress
3	Cell-to-Pack	High Power Applications, Lower Complexity, Faster Equalization, Lower Cost	Higher Switching Voltage / Current Stress, Difficult Modularity
4	Pack-to-Cell	Less Complexity, Easy Modularity, Fast Equalization Speed	Higher Switching Voltage / Current Stress, Larger Size, Lower Efficiency
5	Cell-to-Pack-to-Cell	Very High Power Applications, Lower Complexity, Faster Equalization	High Switching Voltage / Current Stress, Difficult Modularity

The basic solution for cell balancing methods is achieved by equalizing the voltage and charge status between cells connected in a battery pack [22]. Cell balancing based on the working principle of the balancing circuit is typically categorized into two types: 1) active cell balancing and 2) passive cell balancing. A detailed explanation of cell balancing techniques is shown in Figure 4.

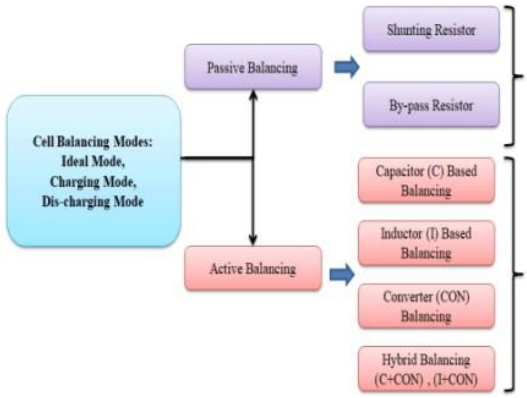

Figure 4 Cell balancing techniques using different methods.

Active cell balancing is used to transfer energy between cells via inductors and capacitors. Converters are used to provide the correct wave width. The active balancing circuit is shown in Figure 5.

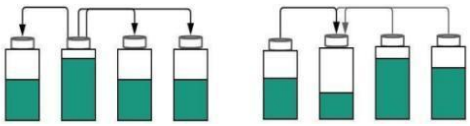

Figure 5 Active balancing circuit.

The active balancing algorithm is shown in Figure 6.

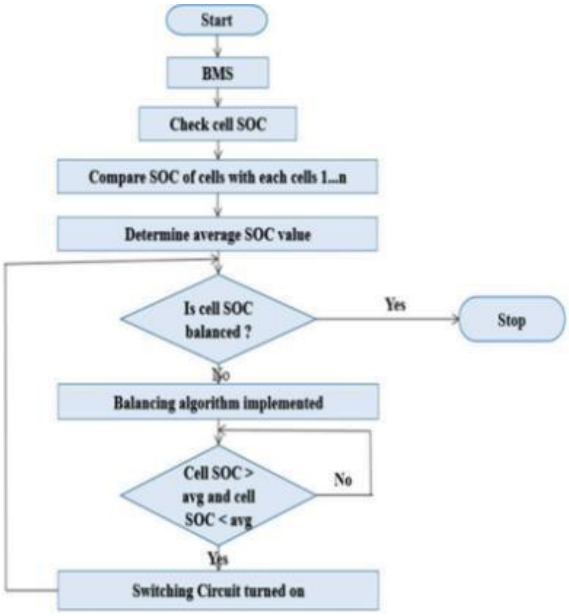

Figure 6 Algorithm for active balancing in battery management systems.

The basis or reference in the form of theories or findings from various previous studies is very necessary and can be used as supporting data. Previous studies are also intended to differentiate the author's research from previous studies. The following table presents the position of previous studies that are related or relevant to the author's research. The position of the author's research in relation to several previous studies is related to the methodology and results of the studies used as references. The novelty of the author's research is its focus on the design of active cell balancing integrated with SOC in lithium-ion batteries.

Table 2. Previous research

Researcher, Research Title, Publication Year	Findings
Neha Khan, Chia Ai Ooi, Abdulrahman	A detailed overview of cell balancing methods and classification based on energy handling method (active and passive balancing), active cell balancing circuits, and control variables. DC-DC converter-based balancing circuits (used to redistribute

Researcher, Research Title, Publication Year	Findings
Alturki, Mohammad Amir, Shreasth, Talal Alharbi A critical review of battery cell balancing techniques, optimal design, converter topologies, and performance evaluation for optimizing storage systems in electric vehicles, Energy Reports 11 (2024) 4999–5032 [15].	the charge among the cells in the battery pack) are the key component in cell balancing as its conversion efficiency affects the overall performance of EVs. Therefore, a detailed overview of different types of DC-DC converter-based cell balancing circuits is provided in this paper. In particular, this paper compares four (isolated/non- isolated) DC-DC converter-based cell balancing circuits, including a duty cycle (bypassed) circuit based on balancing time during both charging and discharging operations. This review paper also covers a detailed review of battery technologies, battery modeling, SoC estimation, and performance optimization of BMS in EV applications. The key is to highlight the characteristics, advantages, and disadvantages, future challenges, and opportunities for advancing electric mobility. Finally, the challenges associated with BMS and battery cell balancing, potential areas for improvement, and future recommendations are provided to embrace the knowledge for the development of high-performance EVs.
Akash Samanta, Sumana Chowdhuri Active Cell Balancing of Lithium-ion Battery Pack Using Dual DC-DC Converter and Auxiliary Lead-acid Battery Journal of Energy Storage Volume 33, January 2021, 102109 [23].	A series of simulation studies were conducted in the MATLAB-Simscape environment to assess the effectiveness of the proposed cell balancing topology. Cell voltage-based and cell SOC-based control logics were developed using MATLAB-State flow diagrams to control the proposed active balancing topology. All results supported that the proposed circuit can implement effective balancing operations during both charging and discharging periods.
Zhang, Z., Zhang, L., Hu, L., Huang, C., 2020. Active cell balancing of lithium-ion battery pack based on average state of charge. Int. J. Energy Res. 44 (4), 2535–2548. https://doi.org/10.1002/er.4876 [16].	An active balancing method for charging and discharging of LiB packs based on average state of charge (SOC) is proposed. Two different active balancing strategies are developed according to the different charging and discharging states of LiB packs. When the LiB pack is charging, a charging balance strategy is en , wherein the battery cells whose SOC is higher than the average SOC of the LiB pack are balanced to increase the charging capacity of the entire LiB pack. When the LiB pack is discharging or in static standby, a discharging balancing strategy is implemented, wherein battery cells with an SOC lower than the average SOC of the LiB pack are balanced to increase the discharging capacity of the entire LiB pack. Experimental results show that the proposed active balancing method can reduce the inconsistency of residual energy between battery cells and improve the charging and discharging capacity of the LiB pack.
Ali, M.U.; Zafar, A.; Nengroo, S.H. Towards a Smarter Battery Management System for Electric Vehicle Applications: A Critical Review of Lithium-Ion Battery State of Charge Estimation. Energies 2019, 12, 446 [22].	In-depth overview of battery SOC estimation methods, focusing on estimation errors and their advantages and disadvantages
Sun, D.; Xu, S.; Li, C. A review of methods for estimating the state of charge of lithium-ion batteries. Battery 2018, 48, 284–287 [24].	Focus on summarizing commonly used lithium- ion battery SOC estimation methods, and analyzing the advantages and disadvantages of various methods
Xiong, R.; Cao, J.; Yu, Q. Critical Review on the Battery State of Charge Estimation Methods for Electric Vehicles. IEEE Access 2018, 6, 1832–1843 [25].	The SOC estimation methods of batteries are reviewed, and three battery models and model- based estimation methods are mainly introduced
Gao, M.K.; Xu, H.L.; Wu, M.B. A review of power battery SOC estimation methods based on equivalent circuit model. Proc. Chin.Soc. Electr. Eng. 2021, 16, 90–102 [26].	The SOC estimation method based on the equivalent circuit model is systematically sorted out and compared with advantages and disadvantages. It also introduces in detail the factors affecting the estimation error and its countermeasures
Zhang, Z.W.; Guo, T.Z.; Gao, M.Y. Review of Research on Estimation Methods of State of Charge of Li-ion Battery for Electric Vehicles. J. Electron.	It focuses on analyzing the main characteristics of five types of estimation algorithms and comprehensively comparing and discussing the advantages and disadvantages of models and their al algorithms.

Researcher, Research Title, Publication Year	Findings
Inf. Technol. 2021, 43, 1803–1815 [16].	
Ma, E.H. A review of SOC estimation models and methods for lithium batteries. China Sci. Technol. Inf. 2021, 17, 36–38 [27].	Analyze the improvement of the battery model and the refinement of the algorithm while considering the temperature.

3. METHODOLOGY

This research uses a Research and Development (R&D) method that focuses on development to expand or deepen a theory or its application in a certain way. In accordance with the type of research, the implementation steps can be designed and arranged in a flowchart, as shown in the following Figure 7.

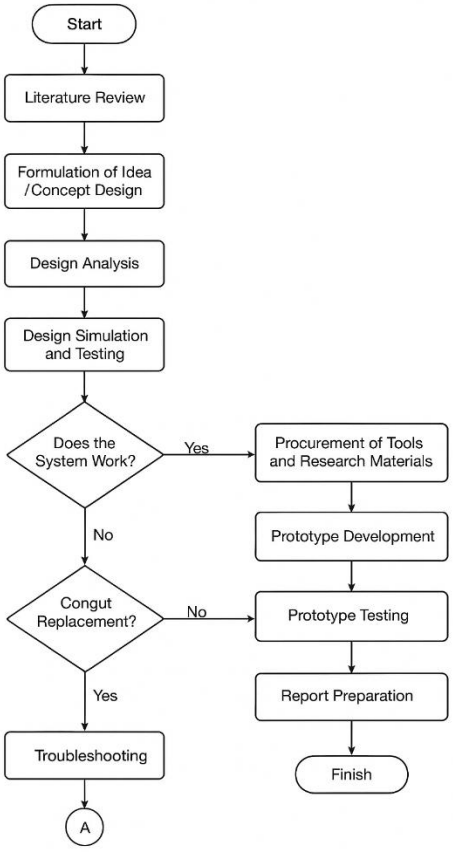

Figure 7 Research flowchart.

3.1. Concepts and Ideas

Cell Balancing design is applied to a 14.8V/2.5Ah battery pack consisting of four 18650 cells equipped with State of Charge (SoC) to ensure voltage balance in each battery cell and monitor the percentage of capacity in each cell. In addition, the system is designed with the addition of overcharge protection, temperature monitor, and short circuit protection devices.

3.2. Hardware Design

Hardware design was carried out to obtain the electronic component scheme that forms the proposed system and to obtain the electronic component arrangement needed to support the control process through a microcontroller, with reference to the following block diagram.

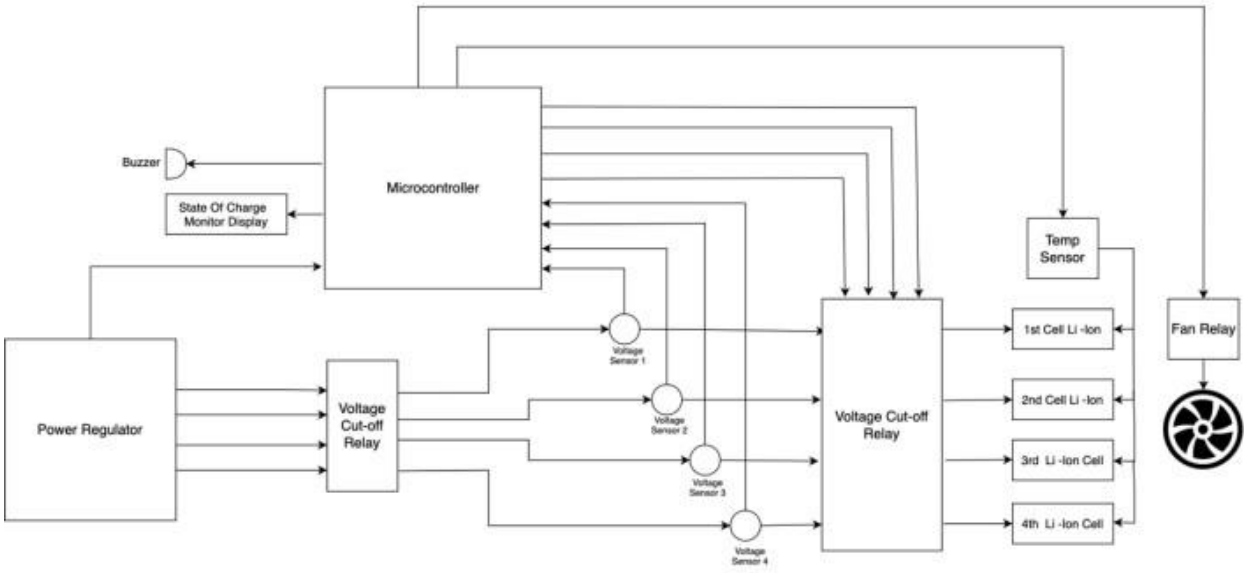

Figure 8 Block diagram of the electronic system.

3.3. Power Regulator

The Power Regulator serves as the power source to supply voltage to each electronic component as activation voltage to meet the power requirements and voltage levels of CMOS/TTL 5V DC and as an auxiliary voltage of 12V by utilizing the role of a central tab transformer 12V/1A as a voltage reducer and an IC regulator 7805 as a 5V regulator, along with capacitors as voltage ripple filters arranged in the configuration shown in the following Figure 9.

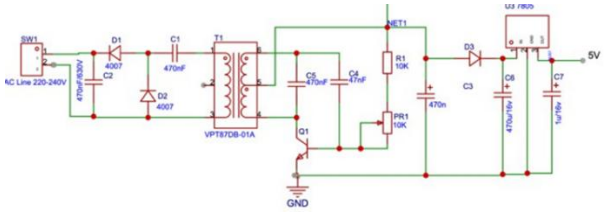

Figure 9 Power regulator configuration layout.

3.4. Microcontroller

The microcontroller used is the Arduino Uno type, which functions as an interface and digital controller that translates commands/executions into electrical quantities used by to monitor voltage, current, and temperature in each cell through the role of sensors. As a medium for data communication between the microcontroller controller and supporting devices (sensors, visual data displays, and sound signallers), the microcontroller is connected to a bus assigned to each pin. The pin configuration is mapped as shown in the following Table 3.

Table 3. Arduino bus and pin mapping

No	Bus	Arduino Pin	Pin Function
1	Bus 0	GND	*Ground*
2	Bus 1	+5V	*5V Supply DC*
3	Bus 2	VIN	*12VDCSupply*
4	Bus 3	SDA	*Serial Data Line*
5	Bus 4	SCL	*Serial Data Clock*
6	Bus 5	D9	*Charge Supply Cell 1*
7	Bus 6	D10	*Charge Supply Cell 2*
8	Bus 7	D11	*Charge Supply Cell 3*
9	Bus 8	D12	*Charge Supply Cell 4*
10	Bus 9	D8	*Charge Trigger Cell 1*
11	Bus 10	D7	*Charge Trigger Cell 2*

No	Bus	Arduino Pin	Pin Function
12	Bus 11	D6	*Charge Trigger Cell 3*
13	Bus 12	D5	*Charge Trigger Cell 4*
14	Bus 13	A0	*Temperature Sensor 1*
15	Bus 14	D3	*Buzzer Trigger*
16	Bus 15	-	-
17	Bus 16	A1	*Temp Sensor 2*
18	Bus 17	D2	*Fan Trigger*
19	Bus 18	-	*FAN Supply*
20	Bus 19	-	-
21	Bus 20	A2	*Voltage Sensor 1 Data*
22	Bus 21	A3	*Voltage Sensor 2 Data*
23	Bus 22	A6	*Voltage Sensor 3 Data*
24	Bus 23	A7	*Voltage Sensor 4 Data*
25	Bus 24	-	*Voltage 4.2V line 1*
26	Bus 25	-	*Voltage 4.2V line 2*
27	Bus 26	-	*Voltage 4.2V line 3*
28	Bus 27	-	*Voltage 4.2V line 4*
29	Bus 28	-	*+Battery Terminal Line*
30	Bus 29	-	*-Battery Terminal Line*
31	Bus 30	-	*-Battery Terminal Line*
32	Bus 31	-	*+Battery Terminal Line*
33	Bus 32	D4	*Terminal Activation Trigger*
34	Bus 33	A0	*Current Sensor*

In addition to being used as the main controller for battery cell monitoring and battery charge estimation, Arduino is also used as a control to display audio and visual information in the form of nominal terminal voltage, cell voltage, charging current, and buzzer sound when a short circuit occurs. The Arduino circuit configuration can be seen in the following Figure 10.

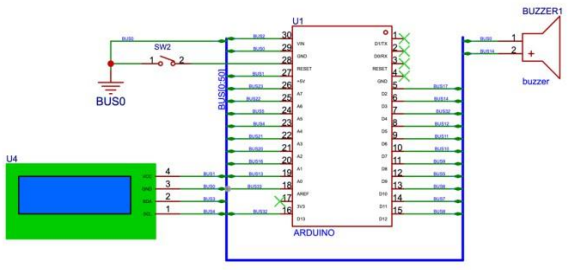

Figure 10 Arduino circuit configuration.

3.5. Battery Pack

The battery used consists of 4 18650 battery cells with specifications of 3.7V/2500 mA connected in series (4S1P), resulting in a terminal voltage of 14.8V with a capacity of 2.5Ah. The Battery Pack is equipped with a voltage sensor, an LM35 temperature sensor, and a DC fan as a battery cooler. A relay is used to support the DC fan to accommodate the 12V drive voltage with the Arduino trigger voltage of 5V. The battery pack configuration is wired according to the schematic shown in the following Figure 11.

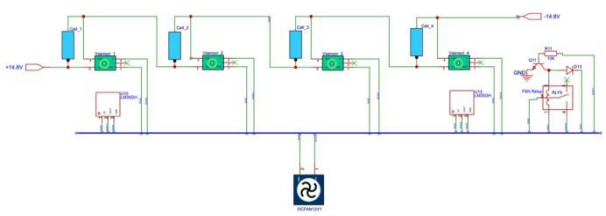

Figure 11 Battery pack circuit diagram.

3.6. Voltage Cut-off Relay

The Voltage Cut-off Relay consists of several solenoid switch components that are electronically activated using trigger voltage from the microcontroller.

The trigger voltage is supplied to the relay when overcharging is detected by the sensor. To support the electronic switching function, the relay is connected to a driver circuit consisting of an NPN BC337 bipolar transistor configured in the saturation region and equipped with an IN400 freewheeling diode. The arrangement of the Voltage Cut-off Relay electronic components can be seen in the following Figure 12.

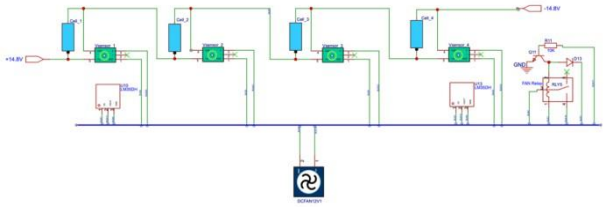

Figure 12 Battery pack circuit diagram.

3.6. Current and Voltage Relay Module

The Current and Voltage Relay Module is a sub-system for overcurrent protection that functions to execute the system shutdown and as an electronic valve that functions to disconnect or conduct the charging voltage to each battery cell. Overcurrent can be detected through the ACS712E sensor with a maximum power rating of 20A. When the detected current exceeds the battery's operating current, the Arduino controller will trigger a signal to disable the operating power via the relay. This module is combined with a step-down converter circuit to reduce the 5V source voltage to 4.2V as the battery cell charging voltage. This module is also equipped with a voltage sensor formed through a voltage divider resistor. This sensor will monitor the charging and discharging process in each cell by comparing the nominal voltage in each cell. In discharging mode, when the cell voltage becomes lower than the nominal voltage of other cells, the relay will activate to charge that cell. Conversely, in charging mode, when the cell voltage becomes higher than the nominal voltage of other cells, the relay will deactivate to stop charging that cell. This mechanism aims to maintain the nominal voltage of each cell relatively equal and balanced (cell balancing). The complete schematic diagram of the current and voltage relay module is shown in the following Figure 13.

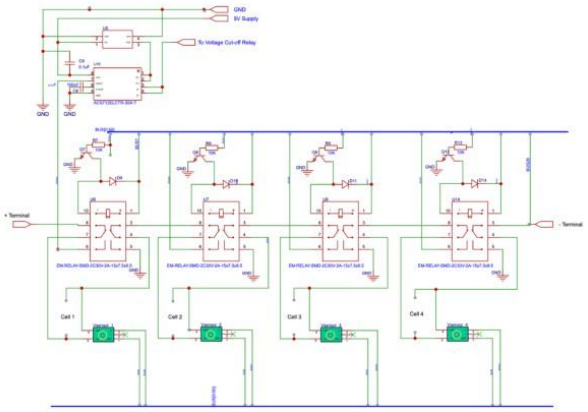

Figure 13 Battery pack circuit diagram.

3.7. Software Design

Software design was carried out to develop algorithms and programming focused on digital signal processing sourced from sensor readings, which were processed to obtain output in the form of relay trigger voltage, current and voltage readings, and buzzer sound information. The program operation process consists of executing commands in machine language (code) through a programming process. The program used in this study was compiled from a procedure consisting of a sequence of steps referring to the crossing process mechanism, resulting in the following logical sequence of steps.

a. Read Battery Status: The initial stage of the program flow is to read the voltage value of each cell for the battery pack terminal voltage calculation process to determine the battery mode (charge/discharge).

b. Read Operation Current: At this stage, the system's operating current value is read and then used as a reference in the shutdown process when there is excess current.

c. Cell Voltage Comparing: This stage involves comparing the voltage value of each cell (Vcell), then determining the lowest voltage (Vmin), and highest voltage (Vmax).

d. Balancing: The process of maintaining cell balance through charging switching according to the operating mode. In the discharging operating mode, when the cell voltage is lower than Vmax, the cell is charged until it reaches the V(max) value.Conversely, in the charging mode,when the cell voltage is greater than V(min), the cell charging process is stopped.

e. Display The Value at this stage, the system will display the terminal voltage, cell voltage, operating current, and battery temperature.

4. RESULT AND DISCUSSION

Scalar *variables* and *physical constants* should be italicized, and a bold (non-italics) font should be used for **vectors** and **matrices**. Do not italicize subscripts unless they are variables. Equations should be either display (with a number in parentheses) or inline. Use the built-in Equation Editor or MathType to insert complex equations.

4.1. Hardware Design

The results obtained through the hardware design and development stages in the previous chapter are detailed as follows.

4.3. Electronic System

The system components described in the block diagram, such as the microcontroller, voltage cut-off relay, current and voltage relay module, buzzer, and other instrument devices, have been integrated into a comprehensive system. This integration produces an overall schematic circuit that can be seen in Figure 4. Details regarding the arrangement and function of each component are explained in detail in Table 4.

Table 4. Bill of materials for electronic components in cell balancing

No	*Component*	*Specification*	*Manufacturer*
1	Arduino Uno R3	ATmega328P/16Mhz chip, 14 digital I/O pins, 6 analog input pins.	Arduino.cc
2	S8050 NPN Transistor	Vce: 25V, Vcb: 40V, Veb: 5V, (Ic): 2A.	Thosiba
3	Relay Module	5V DPDT relay	Omron
4	Diode	1N4007	farnel
5	Buck Converter	12V to 4.2V	NTE Electronics
6	Buzzer	4 to 12V DC; ≤ 85dB; ≤30mA	Farnel
8	Relay	12V, Single Pole Dual Throw	Omron
9	V sensor	Vin: 0-25V DC, Vdet: 0.02445-25V DC, Accuracy: 0.00489V	Infineon
10	Current Sensor	ACS712 5A Range Hall Current Sensor Module For Arduino	Honeywell

The main functions of the components in Table 4 are as follows: the microcontroller acts as the control centre that regulates all system operations; the current and voltage sensors function as readers of current and voltage values; the voltage cut-off relay module operates to cut off the flow of electricity if the voltage exceeds the safe limit; the current and voltage relay module measures and controls the current and voltage; and the buzzer provides an audible signal to indicate certain conditions. Other integrated instruments support various additional functions according to the overall system requirements.

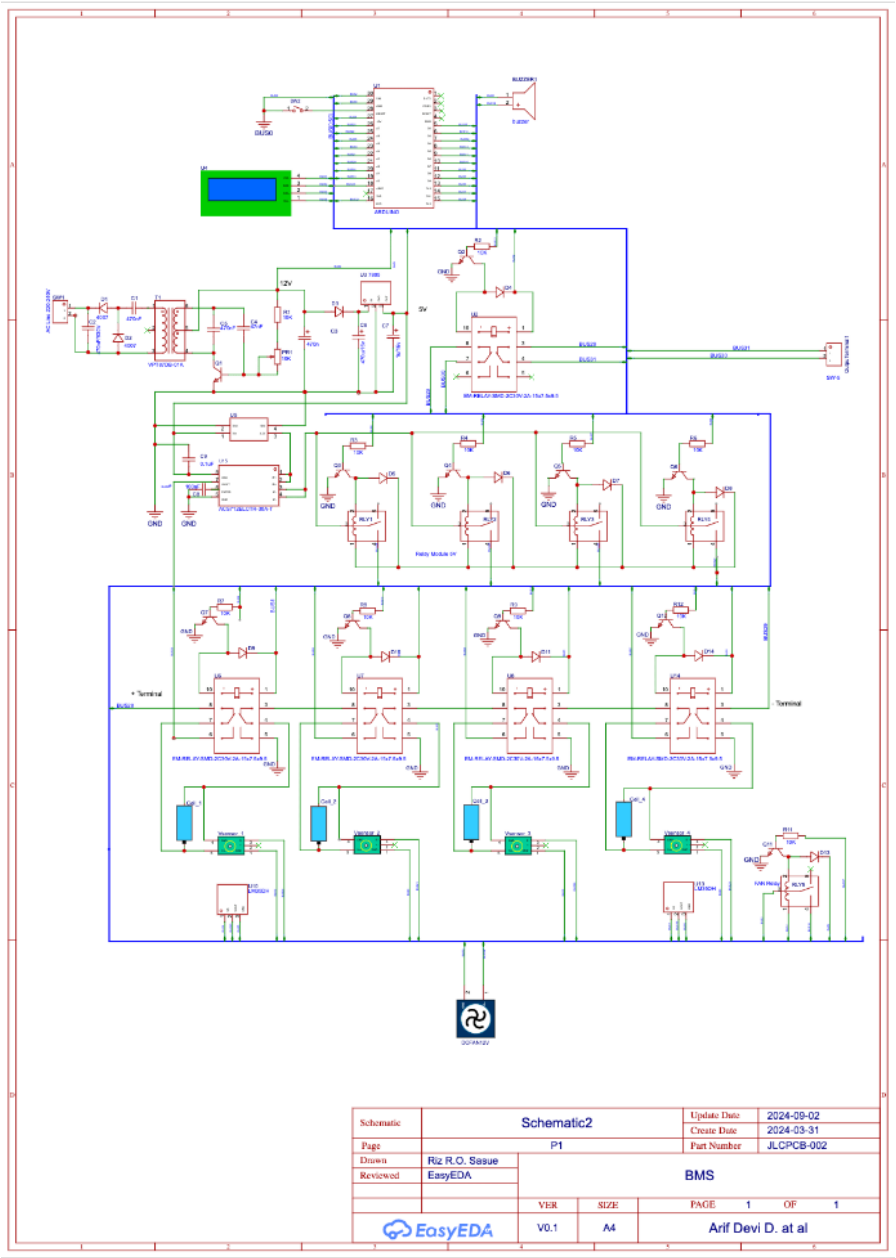

Figure 14 Schematic/wiring diagram.

The schematic/wiring diagram in Figure 14 is then used as a reference in the installation and assembly stages of the electronic components that make up the system, resulting in the installation of hardware components for each subsystem as shown in Figure 15.

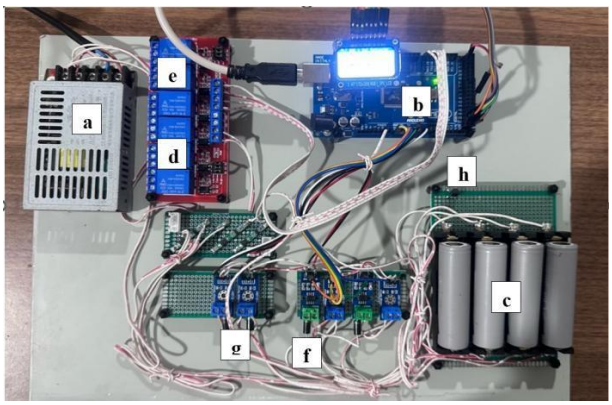

Figure 15 Hardware components: (a) power regulator; (b) microcontroller & LCD Display; (c) battery pack; (d) current and voltage relay module; (e) current and voltage

cut-off relay; (f) current sensor; (g) voltage sensor; (h) temperature sensor; and (i) DC fan.

4.4. Software Design

In accordance with the logical sequence of steps that form the algorithm in sub- section 3.3.3, a flowchart can be obtained which is a visual representation of the logic flow and steps taken by the system in performing its functions as shown in Figure 16.

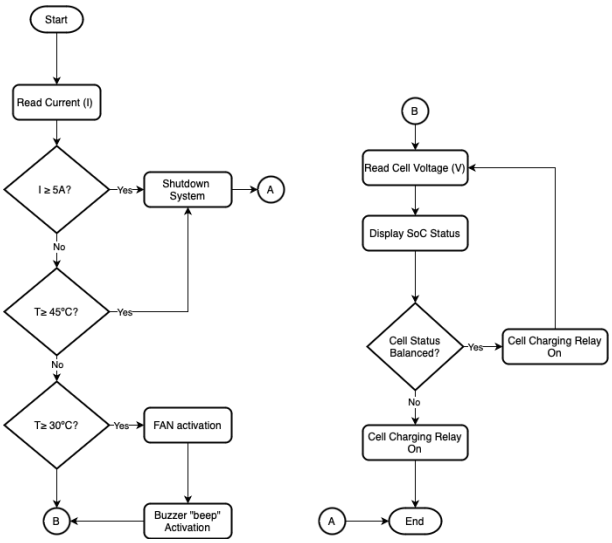

Figure 16 Flowchart software design.

Based on the flowchart in Figure 16, the program code can be written using the syntax of the Arduino Integrated Development Environment (Arduino IDE). The program flow is visually represented in the flowchart in the Arduino programming language based on C language. The code in this programming language is arranged as control commands to the microcontroller to perform the balancing process, monitor the voltage, current, and temperature of the battery cell with the program listing shown in Figure 17 below.

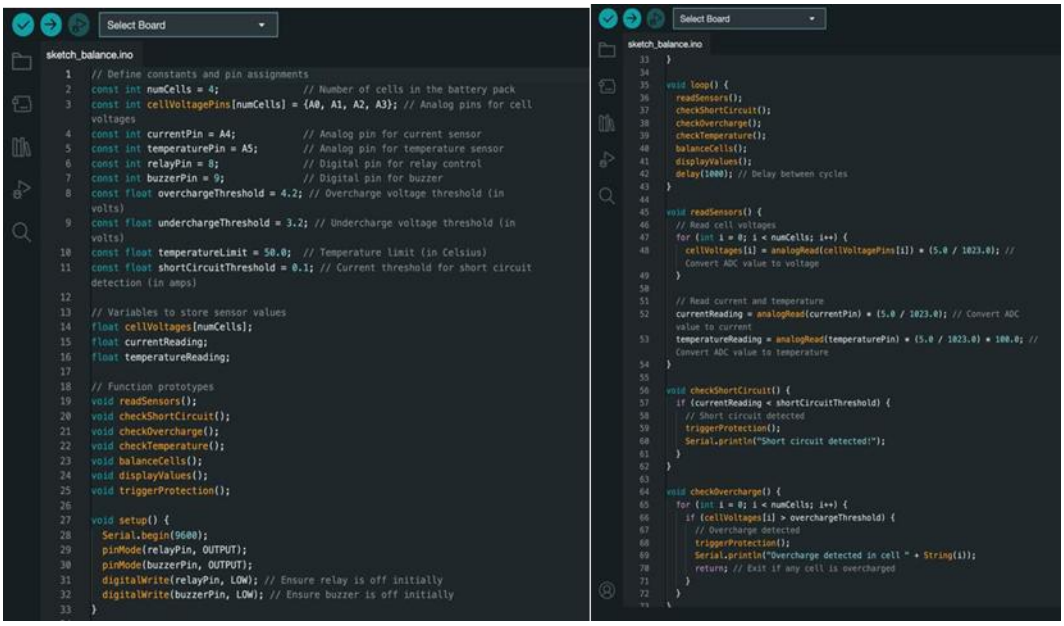

Figure 17 S of arduino IDE programming commands.

The discussion reviews the testing of the research results, specifically the testing of the subsystems that form the overall system of active cell balancing integrated with the SoC estimator in lithium-ion batteries. This begins with testing each subsystem individually, followed by testing the overall system performance, as described below.

4.5. Power Supply Testing

The power supply circuit functions as the power source for all electronic components in the system with terminal voltages of 5V DC and 12V DC. The power supply is also used as a charging voltage source with a nominal value of 4.2V. Testing was carried out by measuring each nominal voltage in an open circuit

condition or without a load and in a loaded condition with a dummy resistor using a digital multimeter. The voltage measurement results are presented in Table 5.

Table 5. Power supply testing

No	Load Condition	No Load *(Open Circuit)*	With Load *(On- Load)*	Deviation
1	Supply 12V$_{DC}$	12.18V	11.97 V	1.72
2	Supply 5V$_{DC}$	5.05V	4.98 V	1.38%
3	Charging Voltage 4.2V	4.24	4.22	0.47

Based on the test results above, the voltage deviation of the power supply circuit under no-load conditions and under load conditions obtained an average deviation value of less than 5% or 1.19%, so the supply voltage from the power supply circuit can be said to be stable and capable of meeting the overall system voltage requirements.

4.6. Voltage/Current Cut-off Relay Testing

The Voltage/Current Relay was tested to ensure the performance of the overcurrent or short circuit protection system in the circuit. The current threshold was set at 5A in accordance with the power supply's current capacity. The test was conducted by applying varying current values ranging from 1A to above 5A to the ACS712 current sensor. s is then performed to observe and measure the voltage at each relay pole socket, Normally Open (NO), Normally Close (NC) as the breaker and connector of the Alternating Current (AC) activation voltage to the power supply, as well as the power supply output terminal as the main electronic power source in the system. The results of the observations and measurements can be seen in Table 6.

Table 6. Testing of voltage/current relay

No	Current Sensor Reading	Trigger Voltage Trigger	Relay Terminal			Power Supply Output		
			Pole	NO	NC	12V	5V	4.2V
1	1A	5.04 V DC	228 V$_{AC}$	228 V$_{AC}$	0 V$_{AC}$	11.98 V$_{DC}$	4.98 V$_{DC}$	4.22 V$_{DC}$
2	2A	5.04 V$_{DC}$	228 V$_{AC}$	228 V$_{AC}$	0 V$_{AC}$	11.98 V$_{DC}$	4.99 V$_{DC}$	4.24 V$_{DC}$
3	3A	5.04 V$_{DC}$	228 V$_{AC}$	228 V$_{AC}$	0 V$_{AC}$	11.98 V$_{DC}$	4.97 V$_{DC}$	4.24 V$_{DC}$
4	4A	5.04 V$_{DC}$	226 V$_{AC}$	226 V$_{AC}$	0 V$_{AC}$	11.97 V$_{DC}$	4.97 V$_{DC}$	4.22 V$_{DC}$
5	5A	5.04 V$_{DC}$	224 V$_{AC}$	224 V$_{AC}$	0 V$_{AC}$	11.97 V$_{DC}$	4.98 V$_{DC}$	4.22 V$_{DC}$
6	6A	0 V$_{DC}$	224 V$_{AC}$	0 V$_{AC}$	224 V$_{AC}$	0V$_{DC}$	0V$_{DC}$	0 V$_{DC}$
7	7A	0 V$_{DC}$	225V$_{AC}$	0 V$_{AC}$	225 V$_{AC}$	0 V$_{DC}$	0 V$_{DC}$	0 V$_{DC}$

Through the observation data in the table above, the ACS712 sensor can read the nominal system current, which is then responded to by the microcontroller by giving a command in the form of a relay voltage trigger for each change in nominal current. When the nominal current is $\leqslant$ 5A, the trigger voltage in the form of a microcontroller command is at High logic (active) with a voltage of 5.04V, so that the voltage from the pole side will be connected to the NO pole and activate the power supply, which is indicated by the appearance of 12V, 5V, and 4.2V terminal voltages. Conversely, when the nominal current is > 5A, representing a short-circuit current, the microcontroller trigger voltage is in Low logic (non-active) with a 0 V voltage, causing the voltage

from the pole side to switch to the NC terminal and the power supply to become inactive, resulting in a system shutdown. These observations confirm that the ACS712 current sensor, microcontroller, and relay function as as expected.

4.7. Current and Voltage Relay Module Testing

Current and Voltage Relay Module Testing was conducted to determine the performance and success of the relay module in executing the switching principle to balance the 4 18650 battery cells. Observations were made during the battery discharge and charging processes with a charging voltage of 4.2V per cell. The relay switching conditions were then observed based on the voltage and current in each cell. The observation data is presented in Table 7.

Table 7. Testing of voltage/current relay

No	Charging Current				Battery Voltage				Relay 1	Relay 2	Relay 3	Relay 4
	Cell 1	Cell 2	Cell 3	Cell 4	Cell 1	Cell 2	Cell 3	Cell 4				
1	0.5A	0.5A	0.5A	0.5A	3.11V	3.18V	2.92V	3.16V	on	on	on	on
2	0.5A	0.1A	0.51A	0.1A	3.46V	3.56V	3.02V	3.52V	on	0ff	on	off
3	0.1A	0.1A	0.5A	0.1A	3.52V	3.74V	3.34V	3.58V	off	off	on	off
4	0.5A	0.1A	0.48A	0.5A	3.53V	3.75V	3.54V	3.58V	on	off	on	on
5	3.72A	3.72A	0.42A	0.38A	3.76V	3.76V	3.69V	3.71V	on	on	on	on
6	0.1A	0.1A	0.31A	0.34A	3.91V	3.92V	3.89V	3.91V	off	off	on	off
7	0.1A	0.1A	0.22A	0.21A	4.22V	4.24V	3.98V	3.91V	off	off	on	on
8	0.1A	0.1A	0.1A	0.1A	4.23V	4.25V	4.22V	4.23V	off	off	off	off

As shown in the table above, when the cell voltage is within the 3V range, the relay activates, allowing the charging current to flow and charge each cell. The voltage of each cell is continuously monitored via the voltage sensor. If any cell has the lowest nominal voltage, the relay remains active on that cell, ensuring the charging current continues to flow. while for other cells with higher nominal voltages, the charging process will stop, indicated by the relay being off, until all cells have the same nominal voltage. This process continues until the battery reaches its maximum voltage of 4.2V. This characteristic demonstrates the ability of the Current and Voltage Relay Module to represent the microcontroller's commands in performing the cell balancing process.

4.8. Cell Balancing Effectiveness Testing

Cell balancing effectiveness testing is conducted to determine the system's success in implementing the principle of balancing battery cells. The test is performed by charging the battery from an empty state to a full state (SoC 0% to 100%) and observing and measuring the cell terminal voltage with a charging current of 1.5 A, a charging voltage of 4.2V, and a charging time of 100 minutes. Voltage measurements were performed using two methods: with and without BMS, to observe the differences before and after using BMS. Additionally, battery temperature was monitored, and the FAN response was observed as a representation of the battery cooling system. The observation results can be seen in Table 8 and Table 9.

Table 8. Observation table for the system without BMS

No	Time (minutes)	Cell 1 Voltage (V)	Cell Voltage 2 (V)	Cell Voltage 3 (V)	Cell Voltage 4 (V)	State of Charge (%)	Temperature (°C)
1	0	3.00	3.00	3.00	3.0	0	25
2	5	3.02	3.08	3.05	3.05	5	25
3	10	3.07	3.11	3.13	3.13	10	26
4	15	3.09	3.14	3.17	3.17	20	27
5	20	3.12	3.15	3.18	3.25	25	28
6	25	3.14	3.17	3.20	3.28	35	30

No	Time (minutes)	Cell 1 Voltage (V)	Cell Voltage 2 (V)	Cell Voltage 3 (V)	Cell Voltage 4 (V)	State of Charge (%)	Temperature (°C)
7	30	3.25	3.21	3.27	3.34	45	31
8	35	3.28	3.33	3.35	3.39	55	31
9	40	3.34	3.38	3.38	3.51	65	32
10	45	3.45	3.41	3.44	3.67	75	27
11	50	3.58	3.53	3.47	3.81	80	27
12	55	3.76	3.67	3.53	3.86	85	29
13	60	3.87	3.73	3.67	3.91	90	26
14	65	3.95	3.86	3.81	3.99	93	27
15	70	4.08	3.95	3.86	4.03	95	27
16	75	4.11	3.97	3.91	4.08	96	28
17	80	4.18	3.99	3.96	4.12	97	28
18	85	4.21	4.07	4.03	4.16	98	28
19	90	4.22	4.09	4.08	4.19	99	28
20	95	4.24	4.12	4.12	4.22	100	28
21	100	4.24	4.22	4.22	4.23	100	27

Table 9. Table of system effectiveness observation with BMS

No	Time (minutes)	Cell 1 Voltage (V)	Cell 2 Voltage (V)	Cell 3 Voltage (V)	Cell 4 Voltage (V)	State of Charge (%)	Temperature (°C)	Fan Response
1	0	3.00	3.00	3.0	3.0	0	25	*off*
2	5	3.02	3.03	3.05	3.05	5	25	*off*
3	10	3.05	3.06	3.07	3.08	10	26	*off*
4	15	3.14	3.13	3.15	3.16	20	27	*off*
5	20	3.16	3.17	3.15	3.18	25	28	*off*
6	25	3.19	3.18	3.20	3.19	35	30	*off*
7	30	3.25	3.23	3.24	3.24	45	31	*on*
8	35	3.32	3.33	3.35	3.33	55	31	*on*
9	40	3.34	3.36	3.37	3.35	65	32	*on*
10	45	3.45	3.43	3.43	3.46	75	31	*on*
11	50	3.58	3.57	3.57	3.57	80	30	*on*
12	55	3.76	3.77	3.75	3.78	85	29	*off*
13	60	3.83	3.83	3.85	3.84	90	28	*off*
14	65	3.95	3.96	3.95	3.99	93	25	*off*
15	70	4.08	4.08	4.08	4.08	95	25	*off*
16	75	4.09	4.10	4.08	4.09	96	28	*off*
17	80	4.18	4.16	4.17	4.17	97	28	*off*
18	85	4.21	4.21	4.20	4.22	98	28	*off*
19	90	4.22	4.22	4.20	4.22	99	27	*off*
20	95	4.24	4.23	4.21	4.21	100	27	*off*
21	100	4.24	4.22	4.23	4.22	100	27	*off*

Tables 8 and 9 show that with a charging voltage of 4.2V during charging, the cell voltage continues to increase over time, indicating the success of the system in distributing the charging power and the ability of each cell to accommodate it. The temperature is seen to continue to increase at 0% SoC at 25ºC until it reaches around 31º at 55% SoC, triggering a temperature sensor reaction that exceeds the threshold (30ºC) with the activation of the cooling system via FAN. The temperature gradually decreases when the SoC is above 55%. This occurs because there is a change in the charging mode of the Li-Ion battery to constant voltage (CV), and the charging current begins to decrease. Through Table 6.4 and Table 6.5, the voltage curve of each cell over time can be visualized, allowing the effectiveness of the BMS system to be seen in Figure 18 and Figure 19.

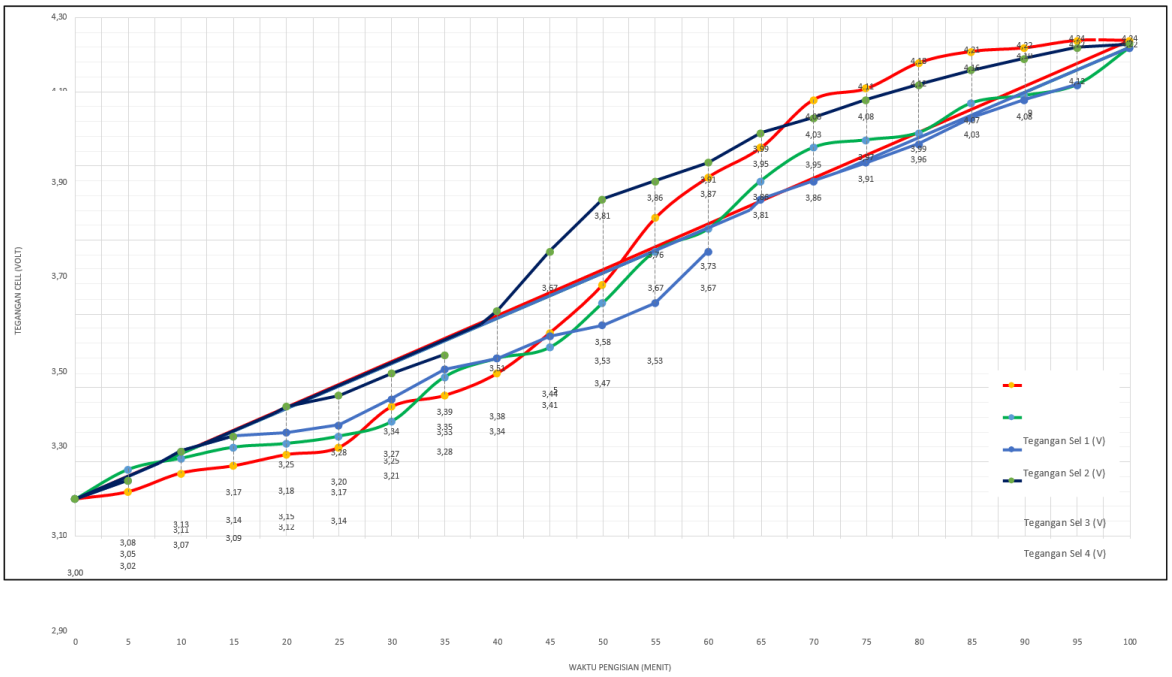

Figure 18 Observation curve of cell voltage over time in a system without BMS.

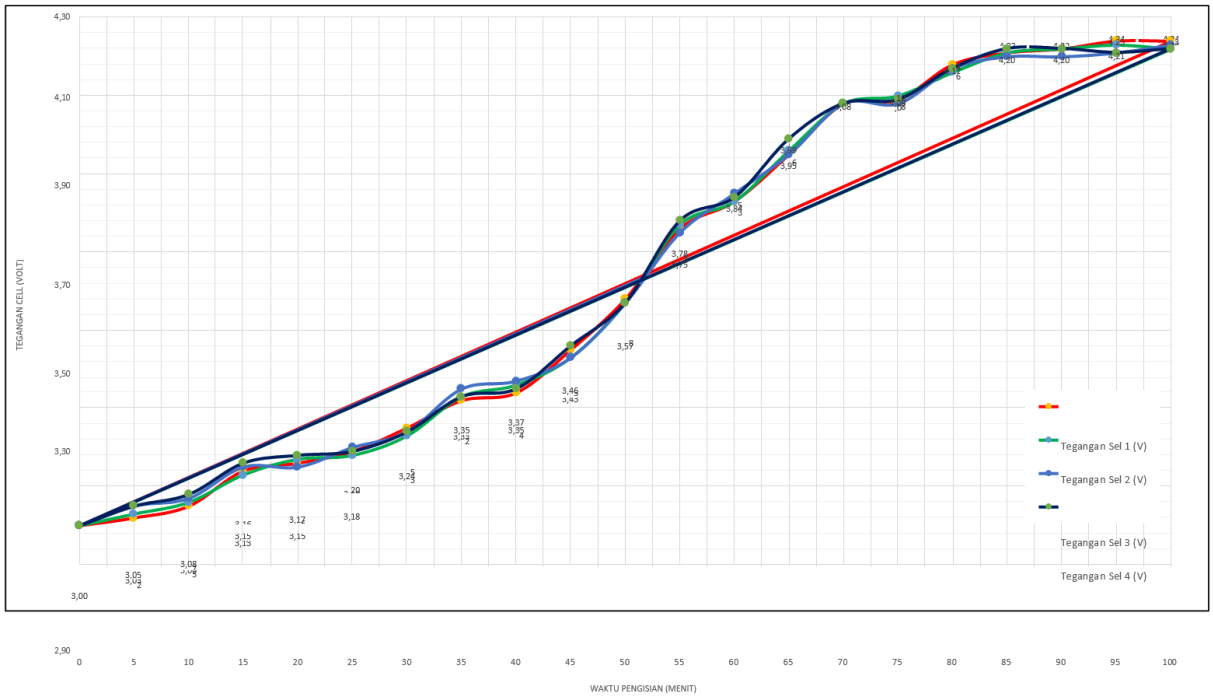

Figure 19 Observation of cell voltage curves over time in a system with BMS (BMS Effectiveness).

Figure 18 shows a visualization of a system without BMS (bypass). A system without BMS does not apply cell balancing, so the curve shows a significant difference with a very wide voltage swing between one cell and another. This condition can cause a decrease in battery performance so that the battery cannot provide maximum power because the weakest cell limits the overall output. Figure 19 shows the cell voltage curve in a system using a BMS. In a BMS system, cell balancing is applied, so that the voltage curve of each cell appears balanced and seems to be on a linear straight line. This is because the low cell voltage will continue to be charged while the cell with the highest voltage experiences a temporary cut-off until the other voltage values have the same nominal voltage or are very close to the highest cell voltage. Through this procedure, all cell values will be balanced, battery temperature tends to be more stable, and maximum power can be achieved to meet the power load requirements.

5. CONCLUSION

The conclusion of this research is that the active cell balancing design integrated with the SoC estimator in lithium-ion batteries shows results in maintaining capacity balance between battery cells, with the main objectives of extending battery life and improving battery performance. Active cell balancing integrated with the SoC estimator produces more accurate measurement performance of the battery's charge level in real-time, providing advantages in battery management, reducing wasted energy, and ensuring more optimal power distribution among battery cells.

REFERENCES

[1] M. S. H. Lipu *et al.*, "A review of state of health and remaining useful life estimation methods for lithium-ion battery in electric vehicles: Challenges and recommendations," *J. Clean. Prod.*, vol. 205, no. 2018, pp. 115–133, 2018, doi: 10.1016/j.jclepro.2018.09.065.

[2] A. Pena-Bello, E. Barbour, M. C. Gonzalez, M. K. Patel, and D. Parra, "Optimized PV-coupled battery systems for combining applications: Impact of battery technology and geography," *Renew. Sustain. Energy Rev.*, vol. 112, no. 2019, pp. 978–990, 2019, doi: 10.1016/j.rser.2019.06.003.

[3] R. T. Yadlapalli, A. Kotapati, R. Kandipati, and C. S. Koritala, "A review on energy efficient technologies for electric vehicle applications," *J. Energy Storage*, vol. 50, no. 2022, p. 104212, 2022, doi: 10.1016/j.est.2022.104212.

[4] Y. Wang, R. Pan, C. Liu, Z. Chen, and Q. Ling, "Power capability evaluation for lithium iron phosphate batteries based on multi-parameter constraints estimation," *J. Power Sources*, vol. 374, no. 2018, pp. 12–23, 2018, doi: 10.1016/j.jpowsour.2017.11.019.

[5] F. Luo, H. Huang, L. Ni, and T. Li, "Rapid prediction of the state of health of retired power batteries based on electrochemical impedance spectroscopy," *J. Energy Storage*, vol. 41, no. 2021, p. 102866, 2021, doi: 10.1016/j.est.2021.102866.

[6] Y. Guo and Y. Chen, "Study on SOC estimation of li-ion battery based on the comparison of UKF algorithm and AUKF algorithm," *J. Phys. Conf. Ser.*, vol. 2418, no. 1, pp. 1–7, 2023, doi: 10.1088/1742-6596/2418/1/012097.

[7] D. Li, X. Liu, and Z. Cheng, "The co-estimation of states for lithium-ion batteries based on segment data," *J. Energy Storage*, vol. 62, no. 2023, p. 106787, 2023, doi: 10.1016/j.est.2023.106787.

[8] X. Tang, Y. Zhou, F. Gao, and X. Lai, "Joint estimation of state-of-charge and state-of-health for all cells in the battery pack using 'leader-follower' strategy," *eTransportation*, vol. 15, no. 2023, p. 100213, 2023, doi: 10.1016/j.etran.2022.100213.

[9] C. Wang, S. Wang, J. Zhou, J. Qiao, X. Yang, and Y. Xie, "A novel back propagation neural network-dual extended Kalman filter method for state-of-charge and state-of-health co-estimation of lithium-ion batteries based on limited memory least square algorithm," *J. Energy Storage*, vol. 59, no. 2023, p. 106563, 2023, doi: 10.1016/j.est.2022.106563.

[10] F. Pampel, S. Pischinger, and M. Teuber, "A systematic comparison of the packing density of battery cell-to-pack concepts at different degrees of implementation," *Results Eng.*, vol. 13, no. 2022, p. 100310, 2022, doi: 10.1016/j.rineng.2021.100310.

[11] N. Campagnol, M. Erriquez, D. Schwedhelm, J. Wu, and T. Wu, "Building better batteries: Insights on chemistry and design from China," McKinsey & Company. Accessed: Oct. 21, 2025. [Online]. Available: https://www.mckinsey.com/industries/automotive-and-assembly/our-insights/building-better-batteries-insights-on-chemistry-and-design-from-china

[12] M. Einhorn, W. Rößler, F. V Conte, H. Popp, and J. Fleig, "Charge balancing of serially connected lithium-ion battery cells in electric vehicles," *e i Elektrotechnik und Informationstechnik*, vol. 129, no. 3, pp. 167–173, 2012, doi: 10.1007/s00502-012-0097-x.

[13] X. Y. Mao, "Research on li-ion battery state of charge and active equalization technology," Nanjing

University of Posts and Telecommunications, 2021.

[14] S. Piller, M. Perrin, and A. Jossen, “Methods for state-of-charge determination and their applications,” *J. Power Sources*, vol. 96, no. 1, pp. 113–120, 2001, doi: 10.1016/S0378-7753(01)00560-2.

[15] N. Khan, C. A. Ooi, A. Alturki, M. Amir, Shreasth, and T. Alharbi, “A critical review of battery cell balancing techniques, optimal design, converter topologies, and performance evaluation for optimizing storage system in electric vehicles,” *Energy Reports*, vol. 11, no. 2024, pp. 4999–5032, 2024, doi: 10.1016/j.egyr.2024.04.041.

[16] Z. Zhang, L. Zhang, L. Hu, and C. Huang, “Active cell balancing of lithium-ion battery pack based on average state of charge,” *Int. J. Energy Res.*, vol. 44, no. 4, pp. 2535–2548, Mar. 2020, doi: 10.1002/er.4876.

[17] E. Buchicchio, A. De Angelis, F. Santoni, P. Carbone, F. Bianconi, and F. Smeraldi, “Battery SOC estimation from EIS data based on machine learning and equivalent circuit model,” *Energy*, vol. 283, no. 2023, p. 128461, 2023, doi: 10.1016/j.energy.2023.128461.

[18] H. Zhou, J. Luo, and Z. Yu, “Co-estimation of SOC and SOH for Li-ion battery based on MIEKPF-EKPF fusion algorithm,” *Energy Reports*, vol. 10, no. 2023, pp. 4420–4428, 2023, doi: 10.1016/j.egyr.2023.11.017.

[19] B. Balasingam, M. Ahmed, and K. Pattipati, “Battery management systems-challenges and some solutions,” *Energies*, vol. 13, no. 11, pp. 1–19, 2020, doi: 10.3390/en13112825.

[20] Z. B. Omariba, L. Zhang, and D. Sun, “Review of battery cell balancing methodologies for optimizing battery pack performance in electric vehicles,” *IEEE Access*, vol. 7, no. 1, pp. 129335–129352, 2019, doi: 10.1109/ACCESS.2019.2940090.

[21] F. Zhao, Y. Guo, and B. Chen, “A review of lithium-ion battery state of charge estimation methods based on machine learning,” *World Electr. Veh. J.*, vol. 15, no. 4, pp. 1–25, 2024, doi: 10.3390/wevj15040131.

[22] M. U. Ali, A. Zafar, S. H. Nengroo, S. Hussain, M. J. Alvi, and H. J. Kim, “Towards a smarter battery management system for electric vehicle applications: A critical review of lithium-ion battery state of charge estimation,” *Energies*, vol. 12, no. 3, pp. 1–33, 2019, doi: 10.3390/en12030446.

[23] A. Samanta and S. Chowdhuri, “Active cell balancing of lithium-ion battery pack using dual DC-DC converter and auxiliary lead-acid battery,” *J. Energy Storage*, vol. 33, no. 2021, p. 102109, 2021, doi: 10.1016/j.est.2020.102109.

[24] D. Sun, S. Xu, and C. Li, “A review of methods for estimating the state of charge of lithium-ion batteries,” *Battery*, vol. 48, no. 2018, pp. 284–287, 2018.

[25] R. Xiong, J. Cao, Q. Yu, H. He, and F. Sun, “Critical review on the battery state of charge estimation methods for electric vehicles,” *IEEE Access*, vol. 6, no. 1, pp. 1832–1843, 2017, doi: 10.1109/ACCESS.2017.2780258.

[26] M. K. Gao, H. L. Xu, and M. B. Wu, “A review of power battery SOC estimation methods based on equivalent circuit model,” *Proc. Chin. Soc. Electr. Eng*, vol. 16, no. 2021, pp. 90–102, 2021.

[27] W. Longxing, P. Hui, and J. Jiamin, “A review of SOC estimation methods for lithium-ion batteries based on electrochemical model,” *Trans. China Electrotech. Soc.*, vol. 37, no. 7, pp. 1703–1725, 20222.